INFECTION AND IMMUNITY, June 2004, p. 3129–3137 Vol. 72, No. 6
0019-9567/04/$08.00+0 DOI: 10.1128/IAI.72.6.3129–3137.2004

Interleukin-10 Limits Local and Body Cavity Inflammation during Infection with Muscle-Stage *Trichinella spiralis*

Daniel P. Beiting,[1]* Susan K. Bliss,[1] Donald H. Schlafer,[2] Victoria L. Roberts,[1] and Judith A. Appleton[1]

James A. Baker Institute for Animal Health[1] and Department of Biomedical Sciences,[2] College of Veterinary Medicine, Cornell University, Ithaca, New York

Received 25 September 2003/Returned for modification 21 November 2003/Accepted 19 February 2004

The aim of this study was to characterize cellular responses to muscle-stage *Trichinella spiralis*. From its intracellular habitat in muscle, *T. spiralis* secretes potent glycoprotein antigens that elicit a strong systemic host immune response. Despite the magnitude and prolonged nature of this response, nurse cells are rarely destroyed by infiltrating cells. We tested the hypothesis that the anti-inflammatory cytokine interleukin-10 (IL-10) moderates cellular responses to muscle-stage parasites. *Trichinella* larvae colonize the diaphragm in large numbers, prompting us to evaluate regional responses in body cavities in addition to local responses in muscle. Mice deficient in IL-10 demonstrated an exaggerated inflammatory response around nurse cells and in the pleural cavity. The effect of IL-10 was most evident 20 days following muscle infection. The increased intensity of the response in IL-10-deficient mice did not affect parasite establishment or survival. Between 20 and 50 days postinfection, the inflammatory response was diminished in both wild-type and IL-10-deficient mice. Muscle infection also elicited an antibody response, characterized initially by mixed isotypes directed at somatic larval antigens and changing to an immunoglobulin G1-dominated response directed at tyvelose-bearing excreted or secreted antigens. We conclude that IL-10 limits local and regional inflammation during the early stages of muscle infection but that chronic inflammation is controlled by an IL-10-independent mechanism that is coincident with a Th2 response.

Infection by the parasitic nematode *Trichinella spiralis* occurs when meat contaminated with infective, first-stage larvae is consumed and the parasite is released from muscle by digestive enzymes in the host stomach. *T. spiralis* invades the epithelium of the small intestine, where it matures, mates, and reproduces (19). Newborn first-stage larvae (NBL) are released in the epithelium, migrate to the lamina propria, and enter venules (5). Larvae travel via the bloodstream, eventually entering skeletal muscle, where each larva invades a single, terminally differentiated muscle cell (myotube) (17). Over a period of 20 days (17), the parasite modifies the infected myotube by inducing reentry into the cell cycle (33), remodeling of the cytoplasmic matrix (17), synthesis of a collagen capsule (46), and formation of a capillary rete around the altered cell (32). These dramatic morphological and biochemical changes in the host cell provide a suitable long-term habitat for the larva, constituting a structure called the nurse cell (43). Although an individual NBL will infect any striated muscle cell, the diaphragm is a preferred site of infection in rodents (50).

Research on muscle-stage *T. spiralis* has focused on elucidating the series of changes that the host muscle cell undergoes following infection (4, 11, 18, 34, 41). The host response to this phase of the infection is not well characterized. Early histologic studies of infected muscle revealed a very limited focus of inflammation surrounding chronically infected muscle cells (23), but the composition and dynamics of the infiltrate remain ill-defined.

The immune system sequesters persistent sources of antigen by establishment of a granulomatous barrier (36, 47, 53). Infections with *Schistosoma mansoni* or *Mycobacterium* spp. are characterized by disease resulting from chronic granulomatous responses to these highly immunogenic pathogens. From its intracellular habitat, *T. spiralis* secretes potent glycoprotein antigens that elicit a strong, systemic host immune response (44), yet local cellular infiltrates are limited. As a first step toward understanding this modulation, we examined the influence of interleukin-10 (IL-10) during synchronized muscle infections of C57BL/6J (wild-type [WT]) mice and B6.129P2-*IL10*^{tm1Cgn} (IL-10$^{-/-}$) mice. IL-10 was first identified as a product of T-helper 2 (Th2) cells and was named cytokine synthesis inhibitory factor (25) because of its ability to inhibit cytokine production by T-helper 1 (Th1) cells. It is now well established that IL-10 interferes with T-cell function indirectly by inhibiting the production of cytokines (26, 40), nitric oxide (14, 28), major histocompatibility complex class II (MHCII) (45), and costimulatory molecules (21) by macrophages. More recently, IL-10 has been identified as a major product of regulatory T cells (29, 42) as well as of a subset of B cells that modulate intestinal inflammation (38).

In this report we describe histochemical, immunohistochemical, and flow cytometric findings that identify the constituents and characterize the architecture of the local cellular infiltrate as well as the cellular response in the pleural and peritoneal cavities. To avoid any complicating influences of IL-10 deficiency on the intestinal stages of infection, we established synchronous muscle infections by intravenous injection with new-

* Corresponding author. Mailing address: James A. Baker Institute for Animal Health, College of Veterinary Medicine, Cornell University, Ithaca, NY 14853. Phone: (607) 256-5647. Fax: (607) 256-5608. E-mail: db225@cornell.edu.

born *T. spiralis* larvae. Our findings reveal a role for IL-10 in limiting inflammatory responses during the early stages of muscle infection by *T. spiralis*. We also provide evidence that sustained control of inflammation during chronic muscle infection is independent of IL-10 and is accompanied by a shift to a Th2 response following completion of parasite development in the muscle.

MATERIALS AND METHODS

Rats and mice. Adult AO strain rats were produced and maintained in the James A. Baker Institute vivarium. Eight-week-old C57BL/6J (WT) and B6.129P2-*IL10*^{tmlCgn} (IL-10$^{-/-}$) mice were obtained from the Jackson Laboratory (Bar Harbor, Maine). IL-10$^{-/-}$ mice had been backcrossed 10 times onto a C57BL/6J background. Mice were maintained in a Bioclean isolation unit (Lab Products Inc, Seaford, Del.) and fed with autoclaved, pelleted ration (5K67; Jackson Laboratory) and acidified water (pH 3). All rodents were housed in the James A. Baker Institute vivarium in accordance with the guidelines of the American Association for Accreditation of Laboratory Animal Care.

Parasite and antigens. *T. spiralis* (pig strain) infectious larvae were recovered from muscles of irradiated AO rats by digestion with 1% pepsin in acidified water (13). The rats had been infected at least 28 days prior to collection of larvae. For recovery of adult worms, the rats were lightly sedated with ether and inoculated by gavage with 6,000 infectious larvae suspended in 0.3 to 0.8 ml of 2% nutrient broth–0.6% gelatin. Six days postinoculation, infected rats were killed by CO_2 inhalation. Intestines were removed, flushed with saline, opened, and incubated for 2 h in saline containing antibiotics (200 IU of penicillin per ml, 200 μg of streptomycin per ml, and 50 μg of gentamicin per ml). Adult worms were recovered on a sterile, 75-μm sieve, washed twice with sterile saline containing antibiotics, and cultured for 24 h in minimal essential medium (MEM) containing 30% fetal calf serum, antibiotics, and 2 mM L-glutamine. NBL were separated from adult worms with a sterile, 75-μm sieve. The larvae were washed twice by gentle centrifugation in serum-free MEM.

Excretory-secretory antigen (ESA) was obtained from overnight cultures of muscle larvae as described previously (2). Somatic antigens from muscle larvae were prepared from whole-worm homogenate as described previously (3).

Experimental design. Mice were given a single intravenous injection (into the lateral tail vein) of 16,000 to 26,000 NBL suspended in 0.25 ml of serum-free MEM. Infection by this route bypasses the intestinal phase of infection, eliminating the intestinal immune response as a confounding variable. In addition, intravenous injection of NBL results in the synchronous development of nurse cells and the host response to muscle infection. Mice were killed by CO_2 inhalation at the times indicated in each experiment.

Total muscle burden estimates and distribution of larvae following parenteral infection. Carcasses of infected mice were skinned, eviscerated, minced, and digested in separate flasks containing 200 ml of 1% pepsin-HCl. A minimum of 100 mature first-stage larvae (L1) were counted from each digestion flask, and the total parasite burden was estimated by extrapolation. In some experiments, anatomic distribution of larvae was determined by digesting the head, diaphragm, upper body, and lower body separately.

Histology. The diaphragm and tongue were fixed in 10% neutral-buffered formaldehyde solution for a minimum of 48 h before being embedded in paraffin. Sections (5 μm) were mounted on glass slides and stained with hematoxylin and eosin (H & E).

Immunohistochemistry. The diaphragm and tongue were embedded in tissue freezing medium (Electron Microscopy Sciences, Ft. Washington, Pa.) and snap-frozen on dry ice. Sections (8 μm) were prepared (Cryocut 1800; Reichert-Jung, Buffalo, N.Y.), mounted on glass slides, and stored at −80°C. The slides were warmed to room temperature and fixed in ice-cold 100% ethanol for 10 min. All incubations were carried out at room temperature for 30 min unless otherwise noted. The slides were washed three times for a total of 5 min in phosphate-buffered saline (PBS) following each incubation. To block endogenous peroxidase activity, the slides were immersed in 0.3% H_2O_2–1% NaN_3 for 15 min. As a general blocking step, sections were incubated in 10% bovine serum albumin (BSA; Sigma Chemical Co., St. Louis, Mo.). Rat antibodies were prepared in 10% BSA. Biotinylated rabbit anti-rat antibody (Vectastain Elite ABC kit; Vector Labs, Burlingame, Calif.) was diluted to 3 μg/ml in a mixture of 10% normal mouse serum and 10% normal rabbit serum. Following incubation with the avidin-biotin complex reagent (Vectastain), sections were incubated for 10 min with metal-enhanced diaminobenzidine substrate (Pierce, Rockford, Ill.), counterstained with Gill's no. 2 hematoxylin (Vector Labs) for 2 min, rinsed in tap water, and mounted with Glycergel (DAKO Corp., Carpinteria, Calif.). Preparations were examined and photographed on BX51 microscope fitted with DP-12 digital camera system (Olympus, Melville, N.Y.).

Antibodies. Unless otherwise indicated, all antibodies were purchased from BD Pharmingen (San Diego, Calif.). Immunohistochemistry experiments employed rat monoclonal antibodies specific for mouse CD8β (clone 53-5.8), CD45R/B220 (clone RA3-6B2), and CD45 (clone 30-F11). Monoclonal antibodies specific for CD4 (clone GK1.5; American Type Culture Collection [ATCC], Manassas, Va.) and MHCII (clone M5/114.15.2; ATCC) were purified from hybridoma supernatants by affinity chromatography (protein G-Sepharose; Pharmacia Biotech, Uppsala, Sweden) as described previously (8). Flow cytometric analyses employed Cy-Chrome-conjugated anti-T-cell receptor β-chain (clone H57-597), allophycocyanin-conjugated anti-CD45R/B220 (clone RA3-6B2), and phycoerythrin-conjugated CD11b (clone M1/70). The specificity of binding was ensured by inclusion of immunoglobulin G2a (IgG2a) conjugated to Cy-Chrome, APC, or PE. Enzyme-linked immunosorbent assay (ELISA) experiments utilized rat monoclonal antibodies specific for mouse IgG1 (clone A85-1), IgG2a (clone R19-15), IgG2b (clone R12-3), IgG3 (clone R40-82), and IgM (clone R6-60.2). Isotype-specific antibodies were detected with horseradish peroxidase-conjugated mouse monoclonal antibody directed against rat Ig kappa light chain (clone G16-510E3).

Preparation of single-cell suspensions from diaphragm and cavity exudates. The diaphragm was removed and washed with PBS. Adherent and infiltrating cells were recovered by mincing the tissue and digesting it for 15 min at 37°C in collagenase I (Sigma Chemical Co.). Undigested muscle was manually dispersed on a stainless steel tea strainer, using a 12-ml syringe pestle. Cell preparations were pooled from three mice and passed through 70- and 40-μm sieves (Falcon, Oxnard, Calif.). Erythrocytes were lysed with Gey's solution for 5 min on ice. The remaining cells were washed twice with 0.25% BSA in PBS (BSA-PBS), and viable cells were counted following dilution in trypan blue. A ratio was calculated using the total pooled cell number from IL-10$^{-/-}$ mice compared to WT mice. Experiments were repeated three times for uninfected mice and those 100 days postinfection (p.i.) and four times for 20 days p.i. Means were determined for each sampling period and evaluated by Fisher's protected least-significant-difference analysis (alpha level of 0.05).

Pleural exudates were obtained by lavage with 2.5 ml of BSA-PBS. The thorax was gently massaged before fluid was recovered with a 3-ml syringe affixed with a 22-gauge, 1-in. needle. Peritoneal exudates were collected by lavage with 10 ml of BSA-PBS. Fluid was recovered with a 12-ml syringe affixed with an 18-gauge, 1-in. needle. Cell preparations from individual mice were prepared as described above. The mean cell numbers were calculated for groups of four or five mice.

Flow cytometry. Cells were treated with 10% normal mouse serum in PBS for 20 min on ice, stained with fluorescent antibodies for 12 min at room temperature, washed once with PBS, and analyzed with a FACSCaliber flow cytometer (Becton Dickenson, Mansfield, Mass.). For data acquisition, 10^4 events were collected within a gate that included mononuclear leukocytes. Phenotypic analysis was carried out on a gate of the lymphocyte population using CellQuest Software (BD Pharmingen).

ELISA. Parasite-specific immunoglobulins in sera were measured by ELISA. Unless otherwise indicated, incubations were carried out for 1 h at room temperature. Polyvinyl 96-well plates were coated with either somatic antigen (5 μg/ml) or ESA (1 μg/ml) overnight at 4°C. Sera from individual mice were serially diluted threefold, and bound antibody was detected with rat monoclonal antibodies to IgG1, IgG2a, IgG2b, IgG3, and IgM (1 μg/ml) followed by horseradish peroxidase-conjugated mouse anti-rat kappa chain (1 μg/ml). The plates were developed for 30 min with tetramethylbenzidine (TMB) peroxidase substrate (KPL Laboratories, Gaithersburg, Md.) and stopped with 1 M H_3PO_4. Absorbance (450 nm) was measured with an ELISA plate reader (Bio-Tek Instruments, Winooski, Vt.). Titers for each isotype were defined as the reciprocal of the last dilution at which the absorbance was greater than 0.1 U. Geometric mean titers were calculated from groups of four mice.

RESULTS

Anatomic distribution and morphologic development of nurse cells. The anatomic distribution of muscle larvae was similar in WT and IL-10$^{-/-}$ mice. Mice were killed between 8 and 20 weeks postinfection. In WT mice (n = 7), the diaphragm yielded 460 ± 400 larvae, while the head, upper body, and lower body yielded 1,039 ± 797, 4,314 ± 2,894, and 2,532 ± 1,850 larvae, respectively. In IL-10$^{-/-}$ mice (n = 10), the

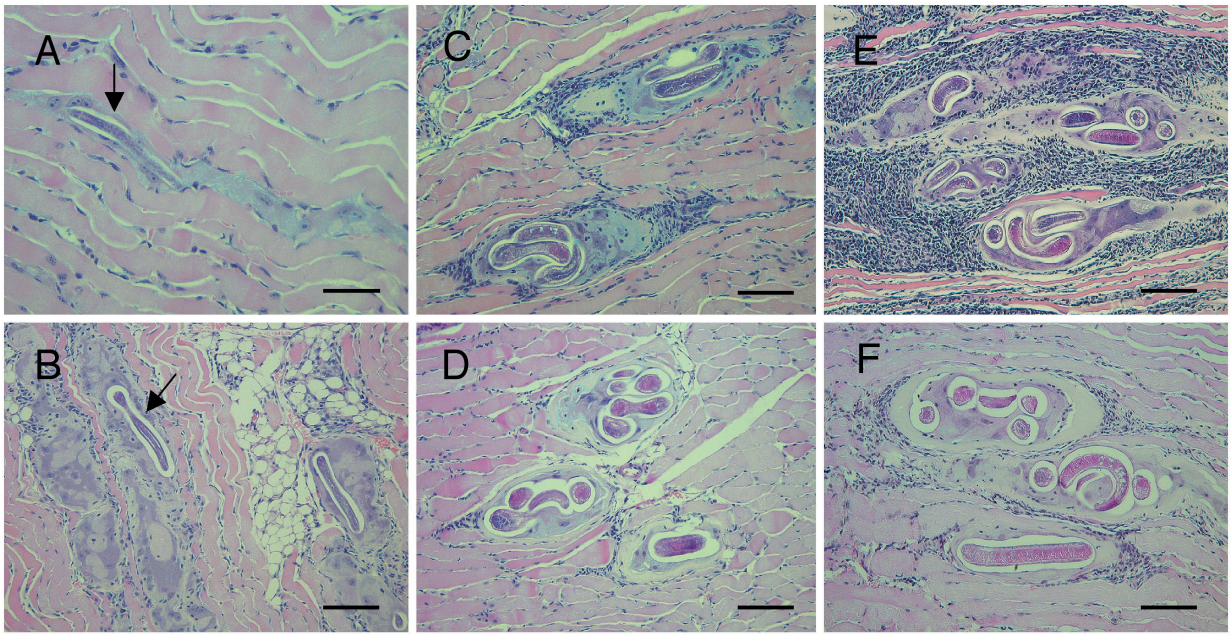

FIG. 1. IL-10 inhibits inflammation during parasite development in muscle. Diaphragms were collected from synchronously infected WT (A to D) and IL-$10^{-/-}$ (E and F) mice, sectioned, and stained with H & E. (A) WT, 5 days p.i.; infected myotubes are basophilic and demonstrate nuclear hypertrophy. (B) WT, 10 days p.i.; cellular infiltrates are evident around infected, hypertrophied muscle cells. (C) WT, 20 days p.i.; focal infiltrates cuff mature nurse cells. (D) WT, 55 days p.i.; attenuated focal infiltrates are seen. (E) IL-$10^{-/-}$, 20 days p.i.; intense focal infiltration by inflammatory cells is seen. (F) IL-$10^{-/-}$, 55 days p.i.; limited focal infiltrates are seen. Arrows denote the location of the *T. spiralis* larva within the muscle cell (A and B). Bars, 50 μm (A), 100 μm (B to F).

diaphragm yielded 395 ± 512 larvae, while the head, upper body, and lower body yielded 987 ± 512, 3,103 ± 1,453, and 2,290 ± 1,408 larvae, respectively. This distribution is similar to that described in orally infected mice of various strains (50).

In general, the development of nurse cells in WT and IL-$10^{-/-}$ mice followed a progression reported previously for mice of various strains (17). Five days after inoculation, occasional basophilic myotubes, each containing a single immature larva in an elongate or serpentine orientation, were observed in the diaphragm (Fig. 1A), tongue, and hind leg muscles (data not shown). Larvae grew approximately twofold between 5 and 10 days p.i. and began to assume a coiled conformation. Significant hypertrophy of infected cells and the initiation of a surrounding capsule were observed by 10 days p.i. (Fig. 1B). At 20 days p.i., infected myotubes were surrounded by thick collagen capsules, had lost all striations, had shortened significantly, and were approximately five times the diameter of adjacent, uninfected myotubes (Fig. 1C). Larvae were mature at 20 days p.i., as evidenced by their resistance to pepsin digestion. The microscopic appearances of larvae and infected cells were not altered between 20 and 55 days p.i. (Fig. 1D).

Development of the inflammatory response in *T. spiralis*-infected muscle. At 5 days p.i., hypertrophy of infected muscle cell nuclei was evident, together with a minimal infiltrate consisting primarily of small lymphocytic foci (Fig. 1A). By 10 days p.i., the inflammatory infiltrate had increased markedly and infected myotubes were cuffed by infiltrating cells (Fig. 1B). Infiltrates were composed largely of mononuclear, fusiform to ovoid cells with ample cytoplasm, interpreted to be macrophages. At 20 days p.i., cuffing was more prominent and the intensity of the inflammatory infiltrate had peaked (Fig. 1C). Eosinophils, scattered plasma cells, and numerous large lymphoblasts were observed; however, macrophages were dominant. Focal areas of necrosis were observed in scattered, dense areas of infiltration. In some instances, infiltrating cells appeared to have entered the nurse cell (Fig. 1C). The volume of the cellular infiltrate began to decline as early as 23 days p.i. (data not shown), continuing until 55 days p.i., when only residual infiltrates remained closely associated with the collagen capsules of infected cells (Fig. 1D).

Influence of IL-10 on the inflammatory response in infected muscle. Comparison of muscles collected 5 days p.i. from WT and IL-$10^{-/-}$ mice revealed no apparent differences in either the composition or the magnitude of inflammation (data not shown). By 10 days p.i., there was a marked increase in the number of inflammatory cells both surrounding individual nurse cells and in the interstitia of IL-$10^{-/-}$ mice versus WT mice (data not shown). The most dramatic differences, however, were apparent at 20 days p.i. (Fig. 1C and E). In IL-$10^{-/-}$ mice (Fig. 1E), there was complete effacement of the interstitial area surrounding some nurse cells, as well as degeneration of several uninfected myotubes incarcerated by infiltrating cells. Nevertheless, by 55 days p.i., inflammation in both groups of mice had resolved (Fig. 1D and F). The composition of infiltrates was similar in the two strains, with a predominance of macrophages and smaller numbers of lymphocytes and eosinophils.

Despite the exaggerated response in the IL-$10^{-/-}$ mice, nurse cell integrity was uncompromised. This was confirmed by assessing whole-body larval burdens. At 20 days p.i., we recov-

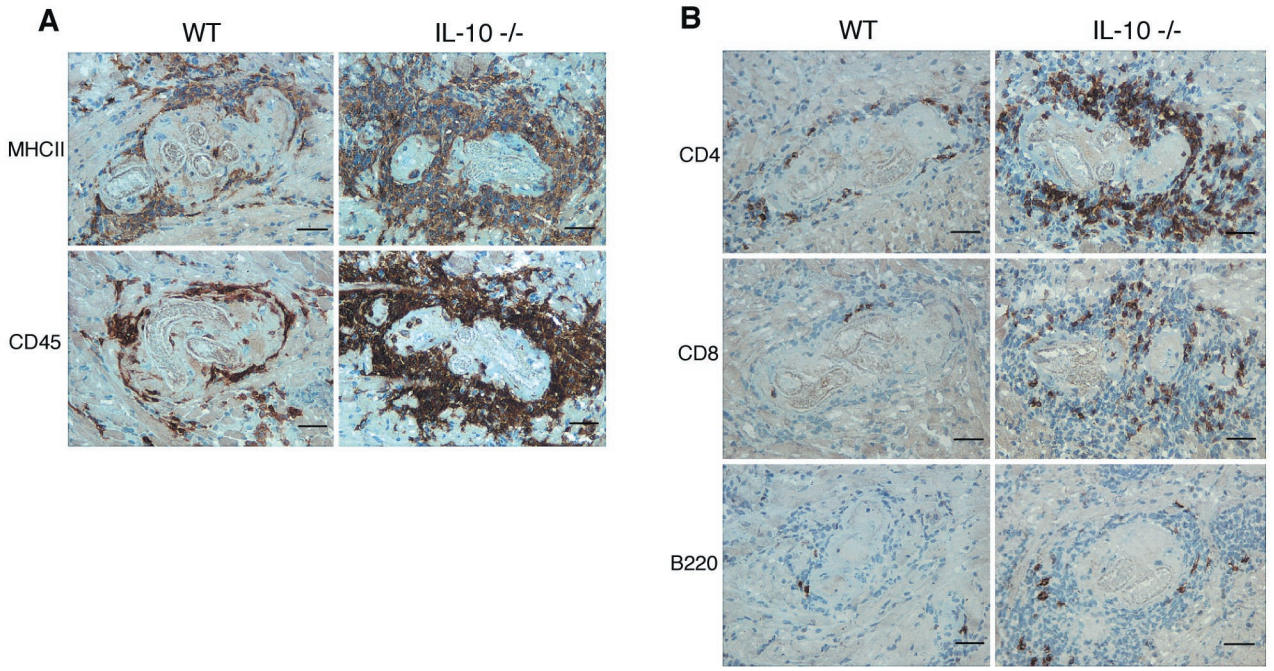

FIG. 2. IL-10 influences the intensity but not the composition of local infiltrates. Sections of tongues recovered from WT and IL-$10^{-/-}$ mice at 20 days p.i. were stained with antibodies. (A) Macrophages ($MHCII^+$, $CD45^+$) dominate the focal response around the nurse cell. (B) Infiltrating lymphocytes are largely $CD4^+$, with fewer $CD8^+$ T cells and rare B cells. Bars, 50 μm.

ered 13,402 ± 2,638 larvae from WT mice (n = 7), compared to 13,862 ± 4,016 larvae from IL-$10^{-/-}$ mice (n = 9). Larva burdens in muscles remained similar at 55 days p.i. (WT [n = 3], 20,826 ± 5,230; IL-$10^{-/-}$ [n = 4], 17,790 ± 4,472). Worms recovered from IL-$10^{-/-}$ mice were motile and morphologically identical to their counterparts recovered from WT mice (normal cuticle structure, coiled conformation, and full stichocyte [secretory organ] development). Although the infectivity of larvae recovered from the muscles of IL-$10^{-/-}$ mice was not directly evaluated, the larvae survived pepsin-HCl digestion, a key criterion in evaluation of physical maturity and infectivity for *T. spiralis*. In addition, larvae resident in muscles of both groups of mice induced high titers of tyvelose-specific antibodies, confirming the secretion or excretion of tyvelose-bearing glycoproteins, a hallmark of infective first-stage larvae. Mice in both groups maintained normal body weight throughout the course of the experiments (data not shown).

Composition of cellular infiltrates associated with nurse cells. Despite the difference in intensity of inflammation in all tissues examined from WT and IL-$10^{-/-}$ mice, the cellular composition of the infiltrates was similar: predominantly $CD11b^+$ cells (data not shown), $MHCII^+$ cells, and $CD45^+$ cells (Fig. 2A), with fewer $CD4^+$ cells and $CD8^+$ cells and rare $B220^+$ cells (Fig. 2B). Small clusters of syndecan-1^+ plasma cells were observed in proximity to nurse cells (data not shown). $MHCII^+$ and $CD45^+$ cells were mononuclear and were presumed to be macrophages.

Expansion of lymphoid aggregates and nodules associated with superficial aspects of the diaphragm following infection with *T. spiralis*. Appreciating the preference for infection of the diaphragm by *T. spiralis* and the unique properties of this muscle with regard to lymph drainage, we explored the inflammatory response at this site in greater detail.

Diaphragms of uninfected WT and IL-$10^{-/-}$ mice were covered with an intact and normal mesothelial layer (Fig. 3i, panels A and B). Small lymphocytic foci were occasionally present in the associated adipose tissue as well as in the mesothelium of uninfected WT and IL-$10^{-/-}$ mice. The mesothelium of WT mice at 20 days p.i. had a mild cellular infiltrate extending into lymphatic lacunae (panel C, arrow). Small lymphoid nodules present in uninfected mice were enlarged in infected WT mice (panel E). Germinal centers were evident in the nodules of WT (Fig. 3ii) and IL-$10^{-/-}$ mice. IL-$10^{-/-}$ mice had larger and more numerous lymphoid nodules (Fig. 3i, panel F), together with a more pronounced cellular infiltrate of the mesothelium (panel D). By 55 days p.i., enlarged lymphoid nodules and infiltrates were no longer evident in either WT or IL-$10^{-/-}$ mice (data not shown).

Quantification of cellular responses in the diaphragms of IL-$10^{-/-}$ mice. To quantify the inflammatory response, we recovered cells by digesting diaphragms with collagenase I. Figure 3iii shows the mean fold increase in diaphragm-associated cell numbers at 0, 20, and 100 days p.i. At 20 days p.i., there was a significant, 3.6-fold increase in the number of cells recovered from diaphragms of IL-$10^{-/-}$ mice compared with those from WT mice (α = 0.05). By 100 days p.i., the ratio had returned to the preinfection value.

Expansion of B- and T-cell populations in the pleural cavities in IL-$10^{-/-}$ mice. To evaluate the body cavity response to muscle infection, cells were enumerated in pleural and peritoneal exudates collected from WT and IL-$10^{-/-}$ mice at 0 and 20 days p.i. WT mice did not undergo significant expansion of

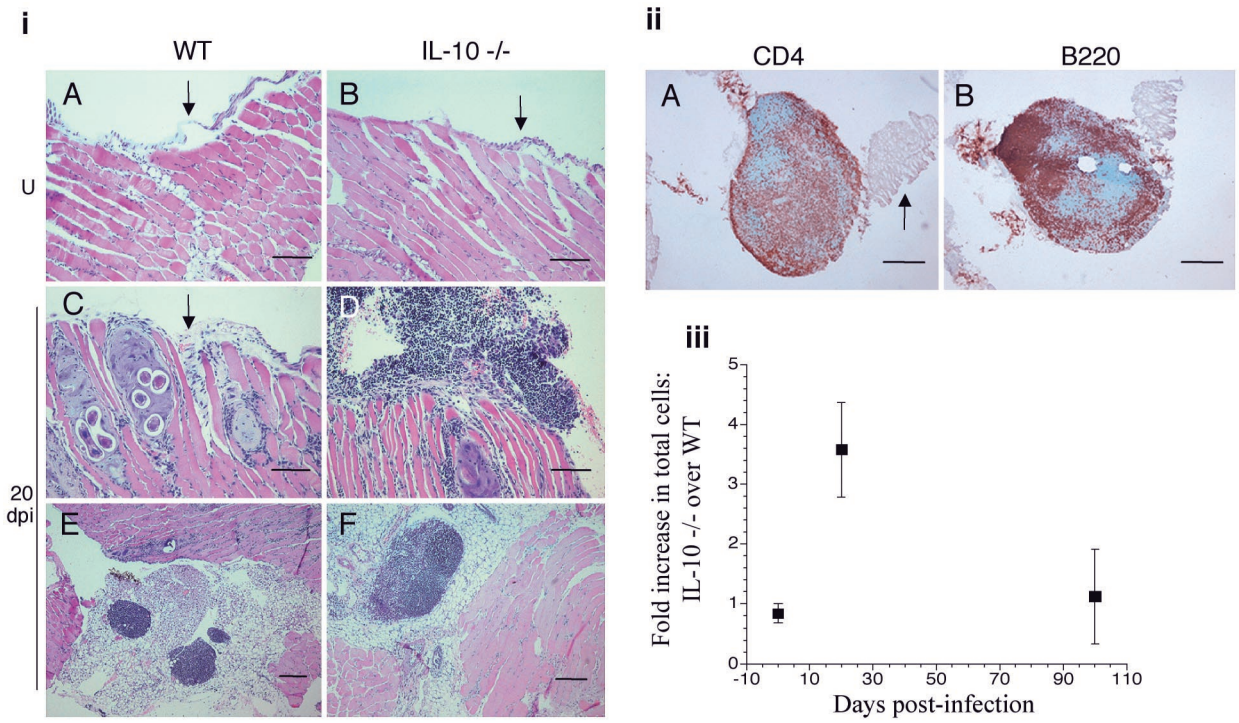

FIG. 3. Attenuation of inflammation at the surface of the diaphragm by IL-10. (i and ii) Sections of diaphragm from 20 days p.i. (dpi) were stained with H & E (i) or with monoclonal antibodies specific for B220 and CD4 (ii). (iii) Alternatively, cells were recovered from diaphragms by digestion and cell suspensions from three mice of each strain were pooled, counted, and expressed as a ratio. (i) (A and B) Normal mesothelia (arrow) cover diaphragms from uninfected WT and IL-$10^{-/-}$ mice; (C) mild cellular infiltration of lymphatic lacuna in the diaphragm of a WT mouse (arrow); (D) pronounced cellular infiltrates and large lymphoid aggregates adhere to the diaphragm of an IL-$10^{-/-}$ mouse; (E) enlarged lymphoid nodule from an infected WT mouse; (F) larger nodule from an infected IL-$10^{-/-}$ mouse. (ii) $CD4^+$ T cells (A) and B cells (B) detected in the germinal center in a nodule from infected WT mouse. The arrow in panel A indicates the diaphragm. (iii) At 20 days p.i., IL-$10^{-/-}$ mice had nearly four times as many infiltrating cells associated with the diaphragm as did WT mice ($P < 0.05$). Relative cell numbers returned to the preinfection level by 100 days p.i. Bars, 100 μm [(i) A to D, (ii) A and B] and 200 μm [(i) E and F]. U, uninfected.

body cavity cell populations in response to infection. IL-$10^{-/-}$ mice demonstrated a greater than threefold expansion in the number of pleural exudate cells ($P < 0.01$) in response to infection (Fig. 4). Uninfected IL-$10^{-/-}$ mice yielded greater numbers of peritoneal exudate cells than did WT mice, but this number did not change significantly on infection ($P = 0.1$)

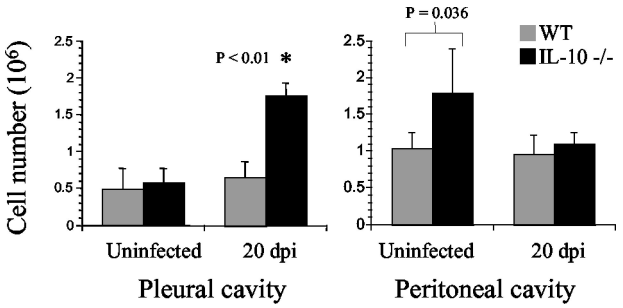

FIG. 4. Cellular response in pleural and peritoneal exudates following infection. At 0 and 20 days p.i. (dpi), pleural and peritoneal exudates were collected and cells were counted ($n = 4$ or 5 mice per strain). Infection induced a three fold increase in the number of pleural exudate cells in IL-$10^{-/-}$ mice ($P < 0.01$). Uninfected IL-$10^{-/-}$ mice yielded greater numbers of peritoneal exudate cells than did WT mice, but this number did not change significantly on infection ($P = 0.1$).

Flow cytometric analysis of exudates from infected IL-$10^{-/-}$ mice revealed modest increases in peritoneal B- and T-cell numbers, while pleural B- and T-cell numbers increased six- and ninefold, respectively (Fig. 5A). In addition to conventional B lymphocytes, or B-2 cells, body cavities possess a population of self-renewing B lymphocytes, so-called B-1 cells (37). B-1 cells can be phenotypically distinguished from B-2 cells by their surface expression of CD11b (6). Evaluation of body cavity $B220^+$ populations for expression of CD11b revealed that IL-10 controlled the expansion of B-2 cells (11-fold) and, to a lesser extent, B-1 cells (4-fold) in the pleural cavity (Fig. 5B). In the peritoneal cavity, IL-10 inhibited the expansion of B-2 cells (threefold) but appeared to be required for maintenance of the B-1-cell population.

Antibody response to muscle infection. The antibody response during oral infections with *T. spiralis* is well documented (1, 16, 44). Our method of infection allowed us to evaluate immunity induced by muscle larvae in the absence of antibody responses to earlier stages of infection. In addition, synchronous arrival of larvae in the musculature may amplify the host humoral response to muscle stage antigens. To evaluate the host response to synchronized muscle infection, IgG1, IgG2a, IgG2b, IgG3, and IgM specific for somatic antigens or ESA were measured at 0, 5, 10, 20, 24, and 55 days p.i. by ELISA (Fig. 6).

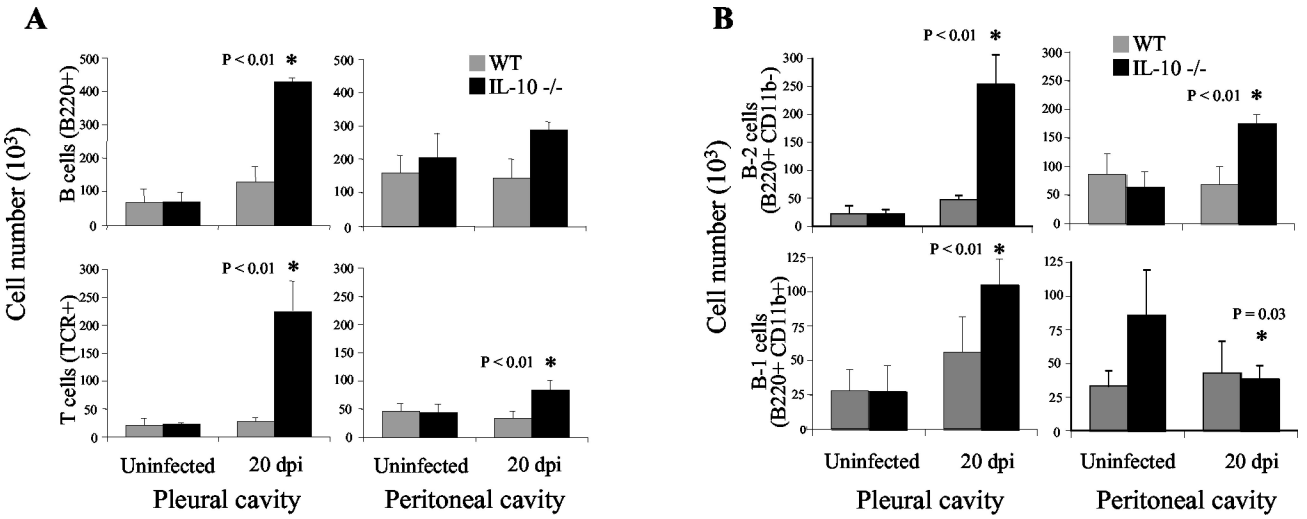

FIG. 5. T and B cells recovered from the pleural and peritoneal cavities during muscle infection. Lymphocytes in pleural and peritoneal exudates ($n = 4$ or 5 mice) were enumerated by flow cytometry following staining with monoclonal antibodies to TCR beta-chain and B220 (A) or, in order to identify B-cell subsets, CD11b and B220 (B). (A) Mice lacking IL-10 showed pleural B- and T-cell populations that were expanded by six and ninefold, respectively. A modest increase in the number of B cells ($P = 0.06$) and a significant increase in the number of T cells ($P < 0.01$) were evident in the peritoneal cavities. (B) Numbers of B-2 cells (11-fold) and B-1 cells (4-fold) were expanded in the pleural cavities of IL-$10^{-/-}$ mice following infection. In the peritoneal cavity, the number of B-2 cells expanded threefold in the absence of IL-10 while the B-1-cell population was diminished twofold following infection. Asterisks mark statistically significant changes (Student's t test). dpi, days p.i.

Comparison of the responses to somatic antigens with those to ESA revealed two distinct phases of antibody production. The first response, mounted from 10 to 20 days p.i., produced antibodies to somatic antigens but not to ESA. The second response, evident at 55 days p.i., was directed at ESA. The early response incorporated IgM, IgG2b, and IgG3. A weak and variable IgG2a response was detected only in IL-$10^{-/-}$ mice. The late response incorporated all the isotypes assayed. Although IgG1 was absent from the early response to somatic antigens, it was dominant in the late response.

Antibody responses in WT and IL-$10^{-/-}$ mice differed only in kinetics, with IL-$10^{-/-}$ mice initiating IgG3 and IgG2a production more rapidly in the early response and IgM more rapidly in the late response. Denkers et al. (16) described the murine antibody response to oral infection with *T. spiralis* as biphasic. The early response is directed against phosphorylcholine, which modifies glycans on somatic glycoproteins (39), while the late response is specific for tyvelose-bearing glycoproteins found in ESA. We analyzed mouse sera from our experiments by Western blotting to determine the specificities of the antibodies produced. We found that sera collected 55 days p.i. contained antibodies specific for tyvelose-bearing glycoproteins. However, antibodies in sera collected 10 to 20 days p.i. did not bind phosphorylcholine-bearing somatic glycoproteins (data not shown). The specificity of antibodies produced between 10 and 20 days p.i. remains unknown.

DISCUSSION

To address the role of IL-10 in the immune response to *T. spiralis* in muscle, we synchronously infected WT and IL-$10^{-/-}$ mice by intravenous injection of NBL. We chose this method to avoid confounding influences of IL-10 on the intestinal stage of infection, since these influences might alter the dose of NBL

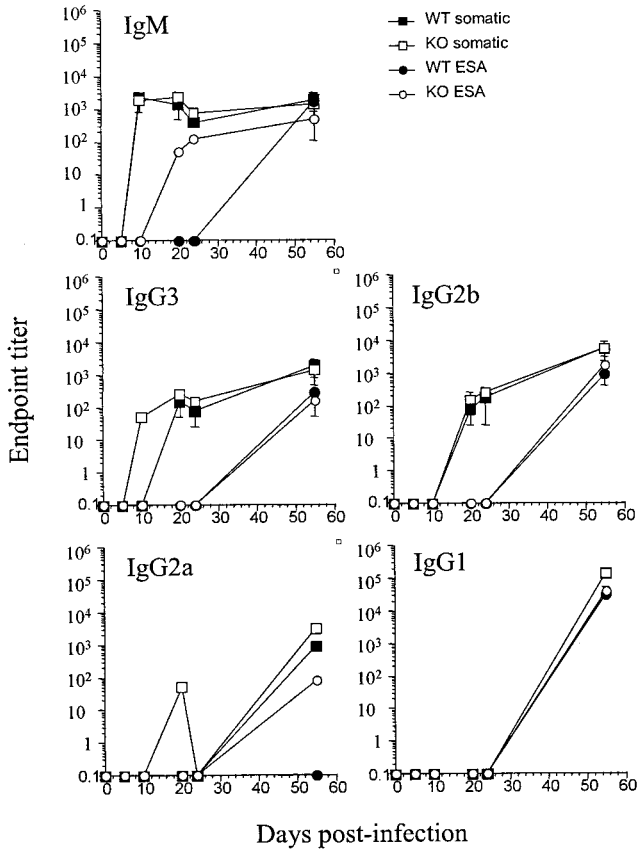

FIG. 6. Antibody response to synchronized muscle infection. Serum titers of IgG1, IgG2a, IgG2b, IgG3, and IgM specific for somatic antigen or ESA in WT and IL-$10^{-/-}$ mice. End-point titers were specified as the reciprocal of the last dilution before the absorbance fell below 0.1 U in ELISA. Geometric means and standard deviations for end-point titers from groups of four mice are shown.

delivered to the muscle. Concurrent investigations in our laboratory showed no effect of IL-10 on the survival of intestinal *T. spiralis*; however, NBL were found to induce large areas of focal necrosis in the livers of IL-$10^{-/-}$ but not WT mice (7). Contradictory results have been reported by Helmby and Grencis (30), who described delayed worm expulsion together with reduced muscle burdens in orally infected IL-$10^{-/-}$ mice. The different outcomes may be due to differences in dose (300 versus 600 larvae given orally) or parasite isolate used in the two studies. Helmby and Grencis concluded that reduced muscle burdens result from gamma interferon-dependent immune response directed against NBL, although it was less clear when or where this influence is effected. The results of our synchronous infections indicate that IL-10 neither promotes nor compromises the survival of larvae in the muscle. This outcome is important to the interpretation of our results, since it demonstrates that immune-deficient and WT mice acquire comparable antigenic loads, eliminating this important variable as an influence on the immune response. The survival of larvae in the presence of the intense inflammation observed in IL-$10^{-/-}$ mice suggests that *T. spiralis* is a highly adapted parasitic organism.

Muscle infection with *T. spiralis* elicited a focal cellular immune response. Nurse cells were surrounded by limited infiltrates in which macrophages were the dominant cell type. Remarkably, parasites survived in close association with macrophages, $CD8^+$ and $CD4^+$ T lymphocytes, and B lymphocytes. It will be important to characterize the functional properties of infiltrating cells in order to understand the basis for parasite survival in what appears to be a hostile environment. Shortly after nurse cell formation was complete, the infiltrates decreased in intensity. We found that IL-10 limited the initial inflammatory response to muscle infection but was not necessary for the down-modulation observed around mature nurse cells. In a similar manner, IL-10 has been shown to control early, but not chronic, granulomatous responses to *Schistosoma mansoni* eggs (57).

The shift from IL-10-dependent to IL-10-independent control of inflammation was coincident with completion of parasite development in the nurse cell, together with the induction of a strong IgG1 response to tyvelose-bearing glycoproteins that are synthesized only by mature first-stage larvae. Class-switching from IgM to IgG1 is controlled by IL-4 (49), the preeminent Th2 cytokine. The induction of an IgG1 response suggests a role for Th2 cytokines in controlling inflammation during chronic infection. A mechanism for targeted activation of Th2 cells by tyvelose-bearing glycoproteins has not been elucidated, although a recent report describes Th2 bias in responses to nematode glycans (52). One outcome of an intense and prolonged IgG1 response to ESA may be modulation of macrophage function. Sutterwala et al. (51) have shown that ligation of the Fc-gamma receptor I, by IgG1 complexed to antigen, inhibits proinflammatory activities of macrophages. Furthermore, the Th2 cytokines IL-4 and IL-13 are key signals in the generation of alternatively activated macrophages, a cell type implicated in the modulation of chronic inflammation in other mouse models of helminth disease (24, 31). There is evidence that *T. spiralis* infection promotes alternative activation of macrophages. Macrophages recovered from the peritoneal cavities of mice infected orally with *T. spiralis* produce the Ym1 protein (12) and are impaired in their ability to control the growth of intracellular *Toxoplasma gondii* (56). These features are consistent with an alternatively activated phenotype. Muscle-stage infection with *T. spiralis* may polarize infiltrating macrophages toward an alternative phenotype, suppressing their destructive properties. In addition, IL-13 inhibits inflammation by enhancing the production of IL-1 receptor antagonist (35, 55) and suppressing the production of proinflammatory cytokines (21, 22). In the context of anti-inflammatory cytokines, consideration must be given to transforming growth factor β, a potent deactivator of macrophage activity in vitro (54) that cooperates with IL-10 in the protection of mice against experimentally induced colitis (27). Our future work will investigate the function of macrophages in chronic *T. spiralis* infection, specifically addressing the interplay among Th2 cells, macrophages, tyvelose-bearing glycoproteins, and specific antibodies.

In our model, the effects of IL-10 are likely to be exerted at the time of immune response activation. Although it is conceivable that IL-10 deficiency causes developmental defects of the immune system, in our experiments IL-10 did not influence the cell types recruited to or retained at the site of infection; instead, it limited the intensity of the response. These observations are consistent with the known effects of IL-10 in suppressing the activity of antigen-presenting cells (9, 20, 21, 26, 40). Our results suggest that IL-10 exerts its anti-inflammatory effect in mice infected with *T. spiralis* by influencing the activities of large numbers of macrophages that surround infected muscle cells.

In addition to moderating inflammation surrounding the nurse cells, we found that IL-10 influenced regional inflammation during muscle infection. The unique physiology of the diaphragm (48) prompted us to examine regional responses during *T. spiralis* infection. We observed cellular infiltrates at the surface of the diaphragm and in the body cavities following infection. Our data indicated that aggregates and nodules observed on the surface of the diaphragm were on the pleural aspect of the muscle. We were able to recover these aggregates by enzymatic digestion and found them to be rich in B and T lymphocytes. When we recovered cavity lymphocytes by lavage, we found that IL-10 limited the expansion of B-2, B-1, and T lymphocytes in the pleural cavity. The magnitude of the response in the pleural cavity most probably was induced by the migration of NBL through the lungs (10). IL-10 controlled the expansion of pleural B-cell populations but did not yield dramatic differences in the levels of parasite-specific serum immunoglobulins, although the production of some isotypes was accelerated in IL-$10^{-/-}$ mice. Currently, we are evaluating the contribution of B lymphocytes to immune modulation in synchronously infected, B-cell-deficient mice.

In summary, we have found that IL-10 limits the initial inflammatory response to muscle infection by *T. spiralis*. This inhibition is evident at the site of infection and in the pleural cavity. Although the source(s) of IL-10 was not identified, candidates include macrophages, $CD4^+$ T cells, and B lymphocytes. Inhibition of inflammation during chronic muscle infection was shown to be IL-10 independent. The transition from IL-10-dependent to IL-10-independent control of inflammation was abrupt, coinciding with parasite maturation and the induction of a dramatic IgG1 response directed at tyvelose-

bearing glycoproteins. Thus, muscle infection by *T. spiralis* serves as a dramatic example of a chronic infection wherein the immune response appears to be controlled in order to promote the survival of both parasite and host.

ACKNOWLEDGMENTS

We thank Paige Adams for helpful comments and Anita Hesser for assistance with manuscript preparation.

This research was supported by grant NIH-AI14490 from the National Institutes of Health. D.B. was supported by training grant T32-AI07643.

REFERENCES

1. **Almond, N. M., and R. M. Parkhouse.** 1986. Immunoglobulin class specific responses to biochemically defined antigens of *Trichinella spiralis*. Parasite Immunol. **8:**391–406.
2. **Appleton, J. A., L. R. Schain, and D. D. McGregor.** 1988. Rapid expulsion of *Trichinella spiralis* in suckling rats: mediation by monoclonal antibodies. Immunology **65:**487–492.
3. **Appleton, J. A., and L. Usack.** 1993. Identification of potential antigenic targets for rapid expulsion of *Trichinella spiralis*. Mol. Biochem. Parasitol. **58:**53–62.
4. **Baruch, A. M., and D. D. Despommier.** 1991. Blood vessels in *Trichinella spiralis* infections: a study using vascular casts. J. Parasitol. **77:**99–103.
5. **Bell, R. G., and C. H. Wang.** 1987. The *Trichinella spiralis* newborn larvae: production, migration and immunity in vivo. Wiad. Parazytol. **33:**453–478.
6. **Berland, R., and H. H. Wortis.** 2002. Origins and functions of B-1 cells with notes on the role of CD5. Annu. Rev. Immunol. **20:**253–300.
7. **Bliss, S. K., A. Alcaraz, and J. A. Appleton.** 2003. IL-10 prevents liver necrosis during murine infection with *Trichinella spiralis*. J. Immunol. **171:** 3142–3147.
8. **Bliss, S. K., Y. Zhang, and E. Y. Denkers.** 1999. Murine neutrophil stimulation by *Toxoplasma gondii* antigen drives high level production of IFN-gamma-independent IL-12. J. Immunol. **163:**2081–2088.
9. **Bogdan, C., Y. Vodovotz, and C. Nathan.** 1991. Macrophage deactivation by interleukin 10. J. Exp. Med. **174:**1549–1555.
10. **Bruschi, F., S. Solfanelli, and R. A. Binaghi.** 1992. Trichinella spiralis: modifications of the cuticle of the newborn larva during passage through the lung. Exp. Parasitol. **75:**1–9.
11. **Capo, V. A., D. D. Despommier, and R. I. Polvere.** 1998. *Trichinella spiralis*: vascular endothelial growth factor is up-regulated within the nurse cell during the early phase of its formation. J. Parasitol. **84:**209–214.
12. **Chang, N. C., S. I. Hung, K. Y. Hwa, I. Kato, J. E. Chen, C. H. Liu, and A. C. Chang.** 2001. A macrophage protein, Ym1, transiently expressed during inflammation is a novel mammalian lectin. J. Biol. Chem. **276:**17497–17506.
13. **Crum, E. D., D. D. Despommier, and D. D. McGregor.** 1977. Immunity to *Trichinella spiralis*. I. Transfer of resistance by two classes of lymphocytes. Immunology **33:**787–795.
14. **Cunha, F. Q., S. Moncada, and F. Y. Liew.** 1992. Interleukin-10 (IL-10) inhibits the induction of nitric oxide synthase by interferon-gamma in murine macrophages. Biochem. Biophys. Res. Commun. **182:**1155–1159.
15. **Ding, L., P. S. Linsley, L. Y. Huang, R. N. Germain, and E. M. Shevach.** 1993. IL-10 inhibits macrophage costimulatory activity by selectively inhibiting the up-regulation of B7 expression. J. Immunol. **151:**1224–1234.
16. **Denkers, E. Y., D. L. Wassom, C. J. Krco, and C. E. Hayes.** 1990. The mouse antibody response to *Trichinella spiralis* defines a single, immunodominant epitope shared by multiple antigens. J. Immunol. **144:**3152–3159.
17. **Despommier, D.** 1975. Adaptive changes in muscle fibers infected with *Trichinella spiralis*. Am. J. Pathol. **78:**477–496.
18. **Despommier, D., W. F. Symmans, and R. Dell.** 1991. Changes in nurse cell nuclei during synchronous infection with *Trichinella spiralis*. J. Parasitol. **77:**290–295.
19. **Despommier, D. D.** 1983. Biology, p. 75–151. *In* W. C. Campbell (ed.), *Trichinella* and trichinosis, vol. 75. Plenum Press, New York, N.Y.
20. **de Waal Malefyt, R., J. Abrams, B. Bennett, C. G. Figdor, and J. E. de Vries.** 1991. Interleukin 10(IL-10) inhibits cytokine synthesis by human monocytes: an autoregulatory role of IL-10 produced by monocytes. J. Exp. Med. **174:** 1209–1220.
21. **de Waal Malefyt, R., C. G. Figdor, R. Huijbens, S. Mohan-Peterson, B. Bennett, J. Culpepper, W. Dang, G. Zurawski, and J. E. de Vries.** 1993. Effects of IL-13 on phenotype, cytokine production, and cytotoxic function of human monocytes. Comparison with IL-4 and modulation by IFN-gamma or IL-10. J. Immunol. **151:**6370–6381.
22. **Di Santo, E., C. Meazza, M. Sironi, P. Fruscella, A. Mantovani, J. D. Sipe, and P. Ghezzi.** 1997. IL-13 inhibits TNF production but potentiates that of IL-6 in vivo and ex vivo in mice. J. Immunol. **159:**379–382.
23. **Drachman, D. A., and T. O. Tuncbay.** 1965. The remote myopathy of trichinosis. Neurology **15:**1127–1135.
24. **Falcone, F. H., P. Loke, X. Zang, A. S. MacDonald, R. M. Maizels, and J. E. Allen.** 2001. A *Brugia malayi* homolog of macrophage migration inhibitory factor reveals an important link between macrophages and eosinophil recruitment during nematode infection. J. Immunol. **167:**5348–5354.
25. **Fiorentino, D. F., M. W. Bond, and T. R. Mosmann.** 1989. Two types of mouse T helper cell. IV. Th2 clones secrete a factor that inhibits cytokine production by Th1 clones. J. Exp. Med. **170:**2081–2095.
26. **Fiorentino, D. F., A. Zlotnik, T. R. Mosmann, M. Howard, and A. O'Garra.** 1991. IL-10 inhibits cytokine production by activated macrophages. J. Immunol. **147:**3815–3822.
27. **Fuss, I. J., M. Boirivant, B. Lacy, and W. Strober.** 2002. The interrelated roles of TGF-beta and IL-10 in the regulation of experimental colitis. J. Immunol. **168:**900–908.
28. **Gazzinelli, R. T., I. P. Oswald, S. L. James, and A. Sher.** 1992. IL-10 inhibits parasite killing and nitrogen oxide production by IFN- gamma-activated macrophages. J. Immunol. **148:**1792–1796.
29. **Hara, M., C. I. Kingsley, M. Niimi, S. Read, S. E. Turvey, A. R. Bushell, P. J. Morris, F. Powrie, and K. J. Wood.** 2001. IL-10 is required for regulatory T cells to mediate tolerance to alloantigens in vivo. J. Immunol. **166:**3789–3796.
30. **Helmby, H., and R. K. Grencis.** 2003. Contrasting roles for IL-10 in protective immunity to different life cycle stages of intestinal nematode parasites. Eur. J. Immunol. **33:**2382–2390.
31. **Hesse, M., M. Modolell, A. C. La Flamme, M. Schito, J. M. Fuentes, A. W. Cheever, E. J. Pearce, and T. A. Wynn.** 2001. Differential regulation of nitric oxide synthase-2 and arginase-1 by type 1/type 2 cytokines in vivo: granulomatous pathology is shaped by the pattern of L-arginine metabolism. J. Immunol. **167:**6533–6544.
32. **Humes, A. G., and R. P. Akers.** 1952. Vascular changes in the cheek pouch of the golden hamster during infection with *Trichinella spiralis* larvae. Anat. Rec. **114:**103–113.
33. **Jasmer, D. P.** 1993. *Trichinella spiralis* infected skeletal muscle cells arrest in G2/M and cease muscle gene expression. J. Cell Biol. **121:**785–793.
34. **Jasmer, D. P.** 1990. *Trichinella spiralis*: altered expression of muscle proteins in trichinosis. Exp. Parasitol. **70:**452–465.
35. **Levine, S. J., T. Wu, and J. H. Shelhamer.** 1997. Extracellular release of the type I intracellular IL-1 receptor antagonist from human airway epithelial cells: differential effects of IL-4, IL-13, IFN-gamma, and corticosteroids. J. Immunol. **158:**5949–5957.
36. **Mariano, M.** 1995. The experimental granuloma. A hypothesis to explain the persistence of the lesion. Rev. Inst. Med. Trop. Sao Paulo **37:**161–176.
37. **Mercolino, T. J., L. W. Arnold, L. A. Hawkins, and G. Haughton.** 1988. Normal mouse peritoneum contains a large population of Ly-1+ (CD5) B cells that recognize phosphatidyl choline. Relationship to cells that secrete hemolytic antibody specific for autologous erythrocytes. J. Exp. Med. **168:** 687–698.
38. **Mizoguchi, A., E. Mizoguchi, H. Takedatsu, R. S. Blumberg, and A. K. Bhan.** 2002. Chronic intestinal inflammatory condition generates IL-10-producing regulatory B cell subset characterized by CD1d upregulation. Immunity **16:**219–230.
39. **Morelle, W., S. M. Haslam, V. Olivier, J. A. Appleton, H. R. Morris, and A. Dell.** 2000. Phosphorylcholine-containing N-glycans of *Trichinella spiralis*: identification of multiantennary lacdiNAc structures. Glycobiology **10:**941–950.
40. **Oswald, I. P., T. A. Wynn, A. Sher, and S. L. James.** 1992. Interleukin 10 inhibits macrophage microbicidal activity by blocking the endogenous production of tumor necrosis factor alpha required as a costimulatory factor for interferon gamma-induced activation. Proc. Natl. Acad. Sci. USA **89:**8676–8680.
41. **Polvere, R. I., C. A. Kabbash, V. A. Capo, I. Kadan, and D. D. Despommier.** 1997. *Trichinella spiralis*: synthesis of type IV and type VI collagen during nurse cell formation. Exp. Parasitol. **86:**191–199.
42. **Pontoux, C., A. Banz, and M. Papiernik.** 2002. Natural CD4 CD25(+) regulatory T cells control the burst of superantigen-induced cytokine production: the role of IL-10. Int. Immunol. **14:**233–239.
43. **Purkerson, M., and D. D. Despommier.** 1974. Fine structure of the muscle phase of *Trichinella spiralis* in the mouse, p. 7–23. *In* C. Kim (ed.), Trichinellosis. Intext Educational Publishers, New York, N.Y.
44. **Reason, A. J., L. A. Ellis, J. A. Appleton, N. Wisnewski, R. B. Grieve, M. McNeil, D. L. Wassom, H. R. Morris, and A. Dell.** 1994. Novel tyvelose-containing tri- and tetra-antennary N-glycans in the immunodominant antigens of the intracellular parasite *Trichinella spiralis*. Glycobiology **4:**593–603.
45. **Redpath, S., A. Angulo, N. R. Gascoigne, and P. Ghazal.** 1999. Murine cytomegalovirus infection down-regulates MHC class II expression on macrophages by induction of IL-10. J. Immunol. **162:**6701–6707.
46. **Ritterson, A. L.** 1966. Nature of the cyst of *Trichinella spiralis*. J. Parasitol. **52:**157–161.
47. **Rumbley, C. A., and S. M. Phillips.** 1999. The schistosome granuloma: an immunoregulatory organelle. Microbes Infect. **1:**499–504.
48. **Shinohara, H.** 1997. Lymphatic system of the mouse diaphragm: morphology and function of the lymphatic sieve. Anat. Rec. **249:**6–15.
49. **Snapper, C. M., F. D. Finkelman, D. Stefany, D. H. Conrad, and W. E. Paul.** 1988. IL-4 induces co-expression of intrinsic membrane IgG1 and IgE by murine B cells stimulated with lipopolysaccharide. J. Immunol. **141:**489–498.

50. **Stewart, G. L., and L. M. Charniga.** 1980. Distribution of *Trichinella spiralis* in muscles of the mouse. J. Parasitol. **66:**688–689.
51. **Sutterwala, F. S., G. J. Noel, P. Salgame, and D. M. Mosser.** 1998. Reversal of proinflammatory responses by ligating the macrophage Fcgamma receptor type I. J. Exp. Med. **188:**217–222.
52. **Tawill, S., L. Le Goff, F. Ali, M. Blaxter, and J. E. Allen.** 2004. Both free-living and parasitic nematodes induce a characteristic Th2 response that is dependent on the presence of intact glycans. Infect. Immun. **72:**398–407.
53. **Toossi, Z.** 2000. The inflammatory response in *Mycobacterium tuberculosis* infection. Arch. Immunol. Ther. Exp. **48:**513–519.
54. **Tsunawaki, S., M. Sporn, A. Ding, and C. Nathan.** 1988. Deactivation of macrophages by transforming growth factor-beta. Nature **334:**260–262.
55. **Vannier, E., R. de Waal Malefyt, A. Salazar-Montes, J. E. de Vries, and C. A. Dinarello.** 1996. Interleukin-13 (IL-13) induces IL-1 receptor antagonist gene expression and protein synthesis in peripheral blood mononuclear cells: inhibition by an IL-4 mutant protein. Blood **87:**3307–3315.
56. **Wing, E. J., J. L. Krahenbuhl, and J. S. Remington.** 1979. Studies of macrophage function during *Trichinella spiralis* infection in mice. Immunology **36:**479–485.
57. **Wynn, T. A., A. W. Cheever, M. E. Williams, S. Hieny, P. Caspar, R. Kuhn, W. Muller, and A. Sher.** 1998. IL-10 regulates liver pathology in acute murine schistosomiasis mansoni but is not required for immune down-modulation of chronic disease. J. Immunol. **160:**4473–4480.

Editor: J. F. Urban, Jr.